Nonlinear Finite-Element Analysis of RC Bridge Columns under Torsion with and without Axial Compression

Tarutal Ghosh Mondal[1] and S. Suriya Prakash, Ph.D.[2]

Abstract: Finite-element (FE) modeling of RC structures under combined loading has received considerable attention in recent years. However, the combination of torsion and axial compression has been rarely studied in spite of its frequent occurrence in bridge columns under earthquake loading. This paper aims at creating a nonlinear FE model to predict the behavior of RC bridge columns under combined torsion and axial compression. A number of circular and square columns were analyzed. The developed FE model was calibrated on local and global behavior through comparison with test data. The overall torque–twist behavior of the members was captured well by the developed FE models. The predicted values of strain in the longitudinal and transverse reinforcement matched closely with the experimental results. An increase in transverse steel ratio was found to increase the torsional capacity and limit the damage of columns under torsion. It was further observed that at a low level of axial compression, the torsional capacity of columns is enhanced. In addition, the FE analysis showed a good agreement on the identification of the damage mechanism and the progression of failure. The shape of the cross section is found to play a major role in the distribution of torsional damage in the columns. Square columns exhibited a more localized damage due to presence of warping, whereas circular columns exhibited damage distributed along their length. **DOI: 10.1061/(ASCE)BE.1943-5592.0000798.**

Author keywords: Finite-element analysis; Reinforced concrete columns; Torsion; Axial compression; Shear flow thickness; Spalling of cover.

Introduction

The damage observed after earthquakes indicates that torsional oscillations are often the cause of distress in buildings and bridges. RC bridge columns with irregular three-dimensional (3D) bridge configurations can undergo significant torsional moments in addition to axial, bending, and shear forces during earthquake events. The addition of torsion is more likely in skewed or horizontally curved bridges, bridges with unequal spans or column heights, and bridges with outrigger bents. Torsion in bridges with outrigger bents occurs because of the eccentricity of the reaction force developed in the footing, which is due to lateral movement of a superstructure under seismic vibration. [If the super structure is subjected to a lateral force (P), reaction force (R) is developed at the footing (Fig. 1). Torsional moment (T) is produced in the beam owing to this eccentric reaction force (R) in the footing]. In skewed bridges, the collision between bridge deck and abutment may cause inplane rotation of superstructures and consequently induces torsion in the bridge columns [Fig. 1(b)].

Torsion effects due to rotation of the superstructure can be significant when shear keys restrain the bridge superstructure at the abutment, and/or if there is a significant decrease in the torsion stiffness in relation to the bending stiffness of the column. Construction of bridges with these configurations is often unavoidable because of site constraints. The force produced in bridge columns because of dead and live loads is primarily axial. Bridges near the earthquake epicenter can be subjected to a significant vertical load (Saadeghvaziri and Fouch 1990), which is typically neglected in design. Lateral seismic loads will cause the single-column bents to translate laterally and rotate slightly when the bridge abutment has significant stiffness. Spread footings and pile footings have adequate torsional restraint to be considered when they are fixed against rotation. As such, the superstructure rotation will cause compatibility torsion in the columns. The load on the columns will, therefore, include axial compression, shear, flexure, and torsion. Axial loads can be considered constant in the absence of a vertical component owing to near-field effects, whereas other loads act cyclically.

Torsional loadings can significantly affect the flow of internal forces and the deformation capacity of RC columns. This, if not considered in design, can influence the performance of vital components of bridges and consequently affect the daily operation of the transportation system. Moreover, the presence of torsional loading increases the possibility of brittle shear–dominated failure, which may result in a fatal catastrophe. However, a review of previously published studies indicates that the torsional behavior of RC members has not been studied in as much depth as the behavior under flexure and shear. The possibility of significant torsional loadings was illustrated in an analytical study carried out to investigate the seismic torsion response of skewed bridge piers by Tirasit and Kawashima (2005). The results from their analysis show that pounding between skewed bridge deck and abutments takes place, resulting in inplane deck rotation that increases seismic torsion in skewed bridge piers. Moreover, they found that the consideration of the locking of bearing movement after failure could extremely amplify the seismic torsion in skewed bridge piers. This necessitates a clear understanding of the effect of torsion combined with bending, shear, and axial compression on the behavior of bridge columns.

[1]Graduate Student, Dept. of Civil Engineering, Indian Institute of Technology, Hyderabad 502205, Andhra Pradesh, India. E-mail: ce13m1023@iith.ac.in

[2]Assistant Professor, Dept. of Civil Engineering, Indian Institute of Technology, Hyderabad 502205, Andhra Pradesh, India (corresponding author). E-mail: suriyap@iith.ac.in

Note. This manuscript was submitted on September 30, 2014; approved on March 31, 2015; published online on June 19, 2015. Discussion period open until November 19, 2015; separate discussions must be submitted for individual papers. This paper is part of the ***Journal of Bridge Engineering***, © ASCE, ISSN 1084-0702/04015037(13)/$25.00.

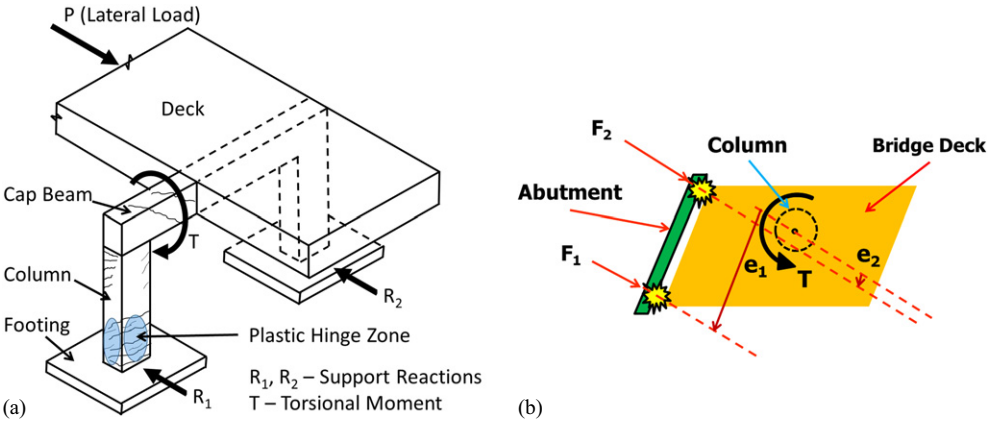

Fig. 1. Torsion in bridge structures: (a) outrigger bent; (b) skew bridge deck

Table 1. Specimen Details

Parameters	Specimen ID				
	H/D(3)-T/M(∞)-1.32%	H/D(6)-T/M(∞)-0.73%	TP-91	TP-92	Missouri square
Section shape	Circular	Circular	Square	Square	Square
Diameter/width (mm)	610	610	400	400	560
Clear cover (mm)	25	25	27.5	27.5	38
Total column height (m)	2.74	4.55	1.75	1.75	3.35
Effective column height (m)	1.83	3.65	1.35	1.35	3.35
Cylinder strength of concrete (MPa)	27.97	37.90	28.3	28.4	34.6
Longitudinal steel yield strength (MPa)	462	462	354	354	512
Transverse steel yield strength (MPa)	457	457	328	328	454
Transverse steel ratio (%)	1.32	0.73	0.79	0.79	1.32
Longitudinal steel ratio (%)	2.1	2.1	1.27	1.27	2.13
Axial force (kN)	600.51	600.51	0	160	0

Seismic torsion in bridges in past earthquakes has been documented (Goel and Chopra 1994), analytically investigated (Isakovic et al. 1998; Meng and Lui 2000; Hurtado 2009; Tirasit and Kawashima 2005; Mondal and Prakash 2015c), and experimentally measured (Johnson et al. 2006; Nelson et al. 2007) by different researchers. In addition, several investigations focused on the response of square (Ogata et al. 2000; Hsu and Wang 2000; Hsu and Liang 2003; Nagata et al. 2004; Otsuka et al. 2004; Tirasit and Kawashima 2005; Mondal and Prakash 2015b), oblong (McLean and Buckingham 1994; Hurtado 2009), and circular (Hurtado 2009; Prakash et al. 2012; Mondal and Prakash 2015a) columns subjected to cyclic and combined torsional loading. Nevertheless, information is scarce on several issues, such as the effect of increasing the transverse reinforcement ratio, the longitudinal reinforcement ratio, the geometry of the cross section, and the effect of axial compression on the torsional response of RC bridge columns. It is essential to expand the knowledge on the behavior of RC members so that the effects of torsion can be clearly understood for developing rational design provisions. A few finite-element (FE) studies in recent years have examined the response of RC columns subjected to combined loading (Mullapudi and Ayoub 2009; Belarbi et al. 2009; Prakash et al. 2010). However, the existing FE models have the limitation of not predicting the postpeak behavior accurately. Moreover, the previously proposed models were validated with test data on global behavior of the specimens alone, with complete disregard to local behaviors such as strain in the reinforcement. In addition, the influence of different sectional parameters (e.g., reinforcement ratio and cross-sectional shape), internal stress distribution, and failure mechanism of the members were inadequately investigated from a FE perspective. To fill this knowledge gap in this area, a FE model is generated in this study to accurately predict the global as well as local behavior of RC columns under combined torsion and axial compression. A number of square and circular columns experimentally tested under torsion with various transverse reinforcement ratios and levels of axial compression (Prakash 2009; Tirasit and Kawashima 2007a, b) were analyzed using full-scale nonlinear FE models. The FE analysis results for overall torque–twist behavior and localized values of strains in the rebar compared favorably with the test results. After calibration of the developed model, a parametric study was carried out to examine the effect of cross-sectional shape, transverse reinforcement ratio, and increasing axial compression. Apart from that, the FE study presented in this paper provides valuable insight into the progression of failure of columns under combined torsion and axial compression. Thickness of shear flow zone and shear stress distribution spanning the cross section are also investigated, which are difficult to measure experimentally. This highlights an important contribution of this paper, because these parameters have not been investigated in detail previously.

Experimental Program

Specimen Details

Five specimens considered in this study include three columns [H/D(3)-T/M(∞)-1.32%, H/D(6)-T/M(∞)-0.73%, and Missouri square] tested at the University of Missouri and another two columns (TP-91 and TP-92) tested at the University of Tokyo. The

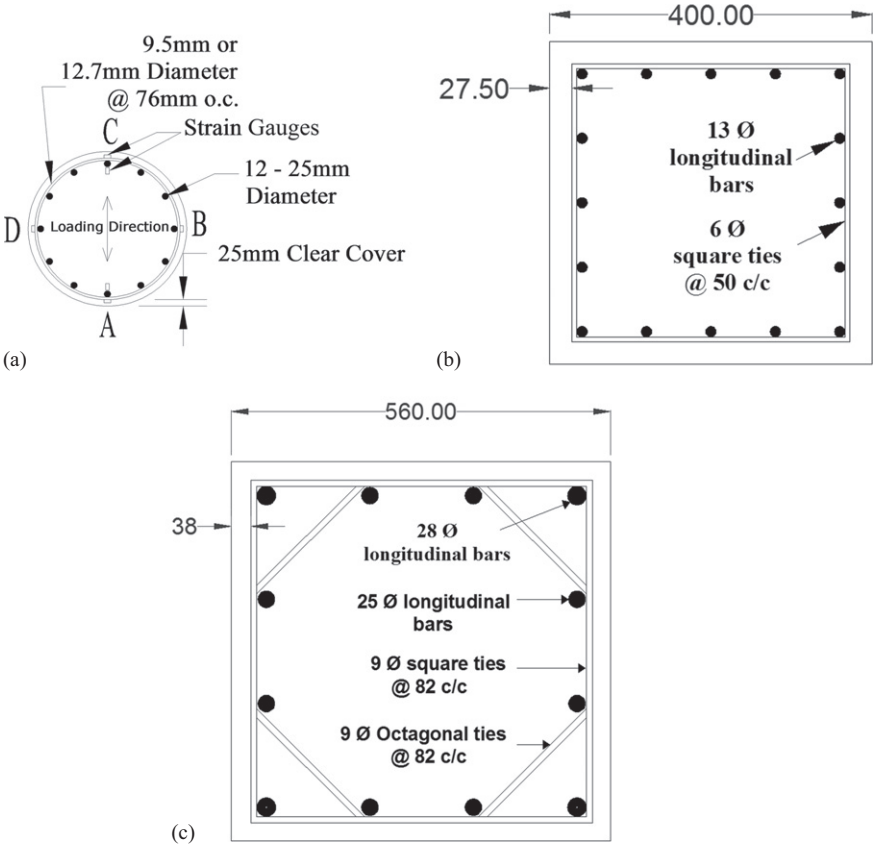

Fig. 2. Cross section of the specimens (dimensions in mm): (a) H/D(6)-T/M(∞)-0.73% and H/D(3)-T/M(∞)-1.32%; (b) TP-91 and TP-92; (c) Missouri square (o.c. = on center; c/c = center to center)

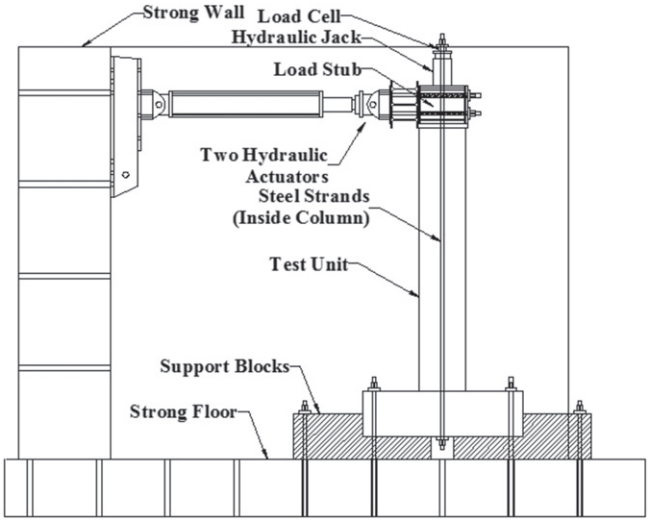

Fig. 3. Test setup (circular columns)

details of the columns are listed in Table 1. The cross-sectional details are shown in Fig. 2.

Test Setup and Loading Protocol

Test data for the specimens tested at the University of Missouri and the University of Tokyo were obtained from Prakash (2009) and Tirasit and Kawashima (2007a, b), respectively. As part of these studies, several columns were tested under cyclic combined loading, including torsion. The test setup for circular columns is shown in Fig. 3. Cyclic torsional loading was generated by controlling two horizontal servocontrolled hydraulic actuators. The axial compressive load was applied by a hydraulic jack on top of the load stubs. The square columns had a similar test setup for applying cyclic torsion. However, in the case of square columns, a time-varying axial compressive load was applied with the help of a vertical actuator attached to the top of the columns.

Finite-Element Study

Material Models

Concrete

Concrete is a quasi-brittle material and has different behavior in compression and tension. The smeared crack approach and damaged plasticity approach are generally used for nonlinear analysis of concrete. In this paper, the damaged plasticity approach has been adopted because it offers a broad potential for matching the simulation results to experimental values (Fink et al. 2007). This is a continuum plasticity–based isotropic damage model, which is used to represent the inelastic behavior of concrete. This model is highly suitable for the analysis of RC structures subjected to monotonic or cyclic dynamic loading under low confining pressure. The details of this model can be found in Jankowiak and Lodygowski (2005), Kmiecik and Kaminski (2011), and SIMULIA (2011).

The values of Young's modulus and Poisson's ratio were provided as elastic properties. For the nonlinear part, compressive stress data are provided as a tabular function of inelastic (or crushing) strain to define the hardening behavior of concrete under

compression. The tension-stiffening option was used to define the strain-softening behavior of concrete after cracking. Tension stiffening can be specified by means of postcracking yield stress and cracking strain values. It helps in approximately modeling of the bond behavior between steel and concrete. The absence of tension stiffening could lead to local cracking failure, which could introduce temporary instability in overall response of the model. Hence, it is important to define tension stiffening from the perspective of numerical stability. The variation of the damage variables with stress states were also specified under tension and compression. Recovery of tensile and compressive stiffness upon load reversal was assumed to be 0 and 95%, respectively (SIMULIA).

The compressive stress–strain model proposed by Vecchio and Collins (1986) was used to model concrete in this study. The behavior is linearly elastic up to about 30% of the maximum compressive strength. Above this point, the stress increases gradually up to the maximum compressive strength. Once it reaches the maximum compressive strength, the curve descends into a softening region, and eventually crushing failure occurs when ultimate strain is reached.

The stress–strain curve for concrete under tension is approximately linearly elastic up to the maximum tensile strength. After this point, the concrete cracks and the strength decreases gradually to zero. Several tension-stiffening models are available to model the strain softening observed in cracked concrete. The exponential model proposed by Greene (2006) has been used in this study to include the tension-stiffening effect. The default values of the failure ratios were taken from the literature (Kmiecik and Kamiński 2011; Chaudhari and Chakrabarti 2012). The dilation angle was assumed to be 36°. The ratio of the ultimate biaxial compressive stress to the ultimate uniaxial compressive stress was taken as 1.16. The absolute value of the ratio of uniaxial tensile stress at failure to the uniaxial compressive stress at failure was assumed to be 0.1, although the default value is 0.09. A default value of 1/3 was considered for the ratio of the principal tensile stress value at cracking in plane stress, when the other nonzero principal stress component attains the ultimate compressive stress value, to the tensile cracking stress under uniaxial tension. The value of the viscosity parameter was assumed to be zero.

Steel

The stress–strain behavior of steel was obtained from coupon tests. Results of the coupon tests conducted on steel used for the circular columns are shown in Fig. 4. Similar results for other specimens can be found in Tirasit (2006) and Prakash (2009). Behavior under compression and tension were assumed to be identical. The yield strength of different steels has been shown in Table 1. Mass density was taken as 7,800 kg/m^3. The modulus of elasticity and Poisson's ratio were assumed to be 200,000 MPa and 0.3, respectively.

Procedure: Dynamic, Explicit

Any quasi-static problem can be solved as a dynamic one with sufficiently slow load increments to produce negligible inertial force. An available explicit integration scheme is used in this study owing to its advantages for highly nonlinear problems (Zimmermann 2001). Robustness in convergence behavior, numerical stability, low computation cost, and suitability for calculation in the postfailure range are the advantages of the explicit integration method. If dynamic analysis is adopted for a static or quasi-static procedure, the ratio of kinetic energy to internal energy (ALLKE:ALLIE) must be less than 0.1, as recommended by Zimmermann (2001). This condition was satisfied for all specimens considered in this study.

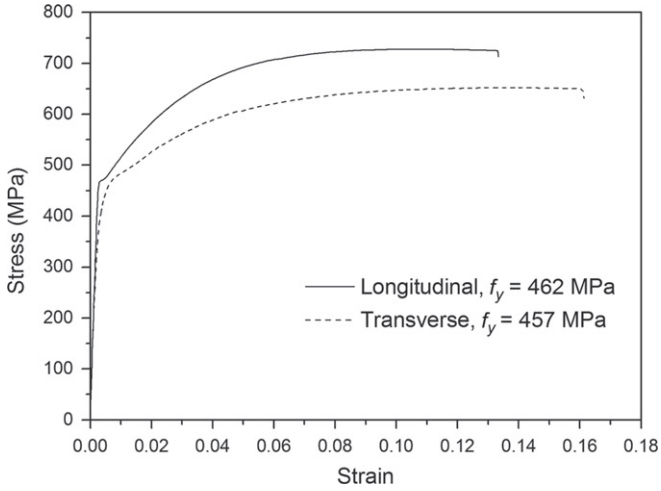

Fig. 4. Coupon test results for steel used in the circular columns

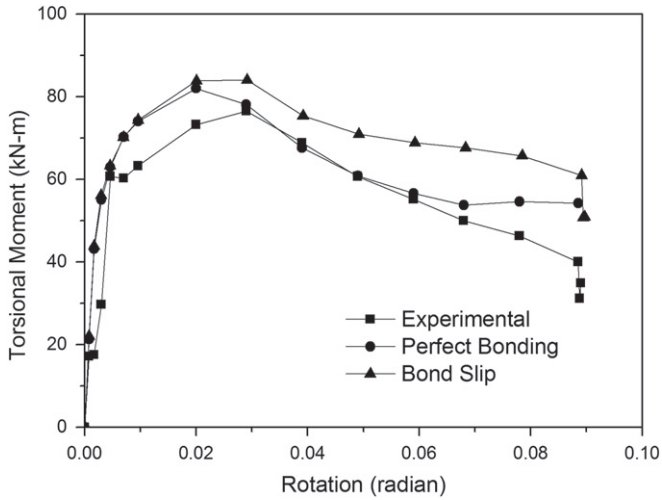

Fig. 5. Bond behavior of steel–concrete interface

Steel–Concrete Interface

The reinforcing steels were modelled as an embedded bar element. Separate truss elements can not only be used for modeling the reinforcement, but they can also be connected to the surrounding concrete elements via the interface elements. This approach is capable of representing the bond stress–slip relations between reinforcement and concrete. To improve the predictions, bond-slip behavior was modeled at the interface between longitudinal steel and concrete using a surface-based contact interaction model. This penalty interaction algorithm uses the Coulomb friction model (SIMULIA) for surface-to-surface interactions. The value of coefficient of friction was assumed to be 0.6, as suggested by Rabbat and Russell (1985). The shear stress limit was taken from Floros and Ingason (2013). Elastic-slip stiffness was obtained from an equation proposed by Delso et al. (2011). The number of parametric studies was carried out to study the influence of bond on torsional behavior. Incorporation of the bond-slip model did not

produce appreciable improvement in the results when compared with the perfect bond model (Fig. 5). The inclusion of bond slip resulted in overestimation of slip and underestimation of stiffness. Hurtado (2009) observed that there was negligible slip during the testing of RC columns under torsion, unlike in flexure, where the slip is considerable. Hence, a perfect bond was considered for modeling the steel–concrete interface in all the models to reduce the computational time and improve the accuracy of the predictions.

Load and Boundary Conditions

One of the key aspects that influence a FE solution significantly is the accurate estimation of load and boundary conditions. In this paper, all degrees of freedom were restrained at the bottom of the columns, whereas the top was free to deform in any mode. The top surface was made rigid using rigid-body constraints, which allow the motion of regions of the assembly to be constrained to the motion of a reference point. The relative positions of the regions that are part of the rigid body remain constant throughout the analysis. A reference point was created at the center of the surface and was assigned as the rigid-body reference point. Motion or constraints applied to the reference point are then applied to the entire rigid part. The angle of rotation was imposed monotonically at the reference point as a function of time in a tabular form. The constant magnitude of axial compressive load was also applied at the same reference point to simulate the experimental study's test conditions.

Meshing

The accuracy of FE results greatly depend on the size of the mesh, the kind of element used, and the order of approximation. Concrete was modeled with the C3D8R element, which is a 3D eight-noded brick element with three translational degrees of freedom at each node. Rotational degrees of freedom are expressed in terms of the translational degrees of freedom. Reduced integration was used to eliminate excess stiffness due to shear locking. Hourglass control was adopted to eliminate the spurious modes. On the other hand, the T3D2 element was used to model the rebar. It is a two-noded 3D truss element with three translational degrees of freedom at each node. The linear elements used in this study require finer mesh, leading to an increase in demand for computer capacity. However, this rise in capacity requirement is offset by the explicit integration scheme, which is compatible to larger mesh sizes. To determine the optimum mesh size for the FE model, a mesh sensitivity analysis was carried out using an element aspect ratio of one. The number of elements was increased, keeping the aspect ratio constant and resulting in smaller mesh sizes. This process was repeated successively until convergence of results was achieved.

Results and Discussion

Validation of the Developed Model

The overall torque–twist behavior of the test specimens was predicted by the developed FE model and compared with the experimental results in Fig. 6. The predictions of the FE model for overall torque–twist behavior were found to be in good agreement with the experimental results. The efficacy of the model in predicting the cracking and ultimate torsional capacity of the tested columns is further illustrated in Table 2. The FE model overestimates the cracking and ultimate torsional capacity, but only to a limited extent. The overestimation can be attributed to the effect of size, material used, and geometric imperfections (Claeson and Johansson 1999), which are not considered in the FE model. The torsional stiffness predicted by the FE model was close to the measured values, particularly in the precracking and postpeak regions. The predicted variation of longitudinal and transverse strain at the midheight of the columns with torsional moment showed a sound match with the experimental observations (Fig. 7). For both square and circular sections, the tie rebar was predicted to yield before the longitudinal rebar, and the same was observed in the experiment. It demonstrates that the developed model is equally effective in predicting the local and global behavior of RC members with fair accuracy.

Overall Torque–Twist Behavior

The overall torque–twist behavior of the square and circular columns is plotted in Fig. 6. The response is essentially linear in the precracking range. After cracking, the torque–twist behavior exhibits a short plateau followed by an increase in resistance at a tangential stiffness equal to a small fraction of the initial stiffness. Similar behavior was observed in previous analytical studies using a softened truss model (Hsu 1968) and modified compression field theory (MCFT) (Mitchell and Collins 1974), which are used extensively for prediction of the torsional response of RC members. Failure of the columns subjected to torsion was governed by diagonal cracking leading to the formation of a torsional plastic hinge near the midheight of the columns (Prakash et al. 2012).

Effect of Axial Compression

The tested square columns used for FE validation had an axial stress of 0 and 1 MPa, and the circular columns had a constant axial stress of 2 MPa. The effect of axial compression on the torsional behavior of square and circular RC columns is shown in Fig. 8. The presence of an axial compressive load delays the tensile stresses in concrete arising from torsion. Thus, the cracking of concrete under diagonal tension is delayed. Consequently, cracking torsional capacity of RC members increases significantly in the presence of a low axial compressive load. Increased torsional moment with axial compressive load causes shear cracks spiraling around the column. This results in a concrete compression field in the form of diagonal struts that will induce uniform tensile stress in longitudinal and transverse reinforcements. If some axial compression is applied together with torsional moment, and assuming that the column section is cracked because of applied torsion, the tension in the longitudinal steel induced by torsion will be reduced by the axial compression. Thus, axial compression loading will produce an effect similar to that of increasing the longitudinal steel content in resisting the applied torsion. This increases the torsional capacity of the section, as observed in Fig. 8. A similar observation was recorded experimentally by Jakobsen et al. (1984) for box columns, Hurtado (2009) for circular columns, and Bishara and Peir (1973) for square columns. In future studies, more test results on columns with different sectional parameters should clarify the effect of axial compression on the torsional capacity of RC columns.

Effect of Transverse Reinforcement

The effect of transverse reinforcement on the torsional moment–twist response of square and circular bridge columns was investigated, and the results are shown in Fig. 9. The increase in the transverse reinforcement ratio increased the peak torsional

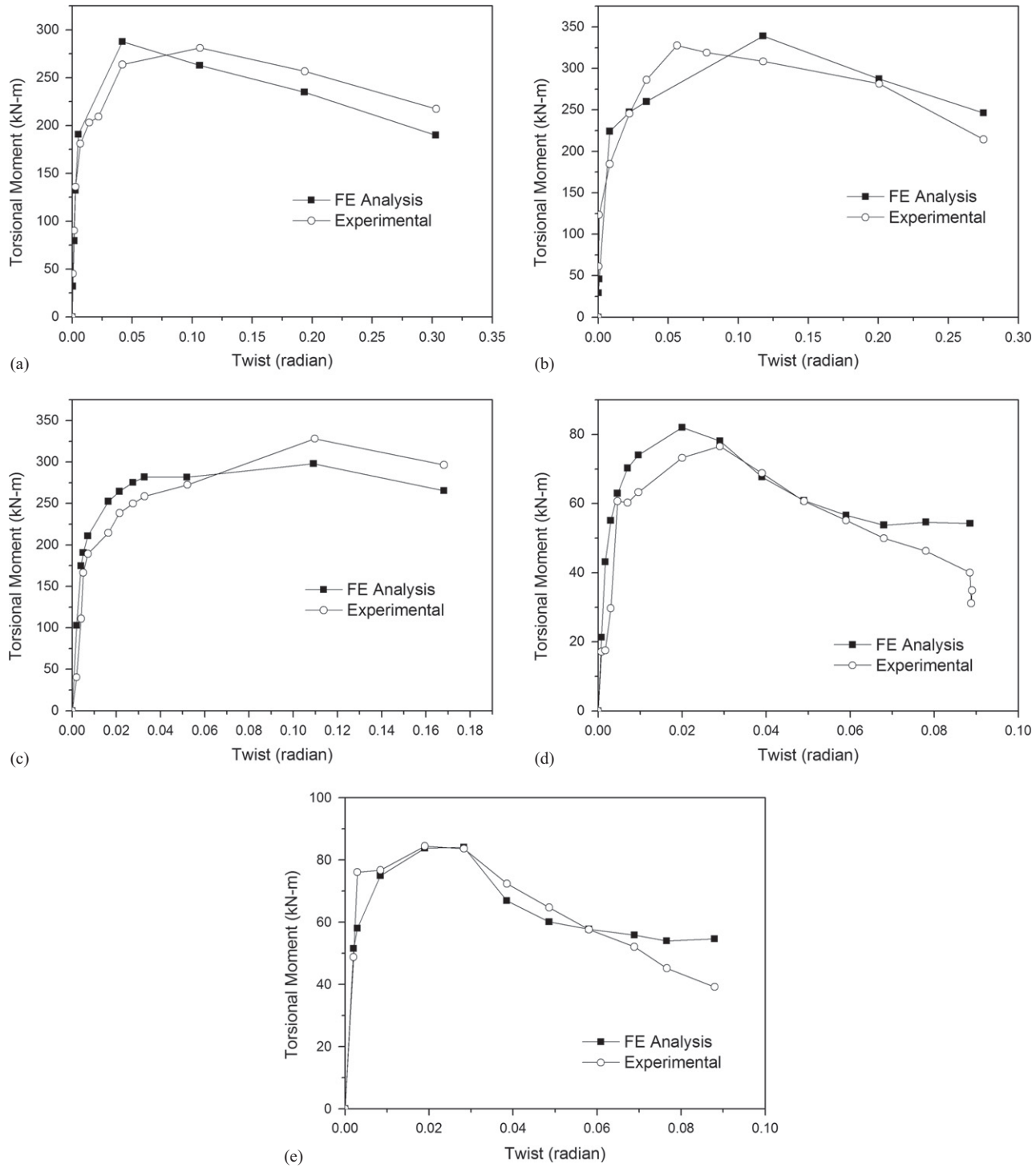

Fig. 6. Overall torque–twist behavior: (a) H/D(6)-T/M(∞)-0.73%; (b) H/D(3)-T/M(∞)-1.32%; (c) Missouri square; (d) TP-91; (e) TP-92

Table 2. Comparison of Predicted Values with Test Data

Parameter	Result	TP-91	TP-92	H/D(6)-T/M(∞)-0.73%	H/D(3)-T/M(∞)-1.32%	Missouri square
Cracking torque (kN·m)	FE analysis (A)	62.9	58.0	190.7	224.1	212.3
	Experimental (B)	60.7	76.6	180.9	184.6	189.3
	A/B	1.04	0.76	1.05	1.21	1.12
Ultimate torque (kN·m)	FE analysis (A)	82.0	84.1	287.7	338.8	283.7
	Experimental (B)	76.6	84.4	281.1	327.5	328.0
	A/B	1.07	0.99	1.02	1.03	0.86

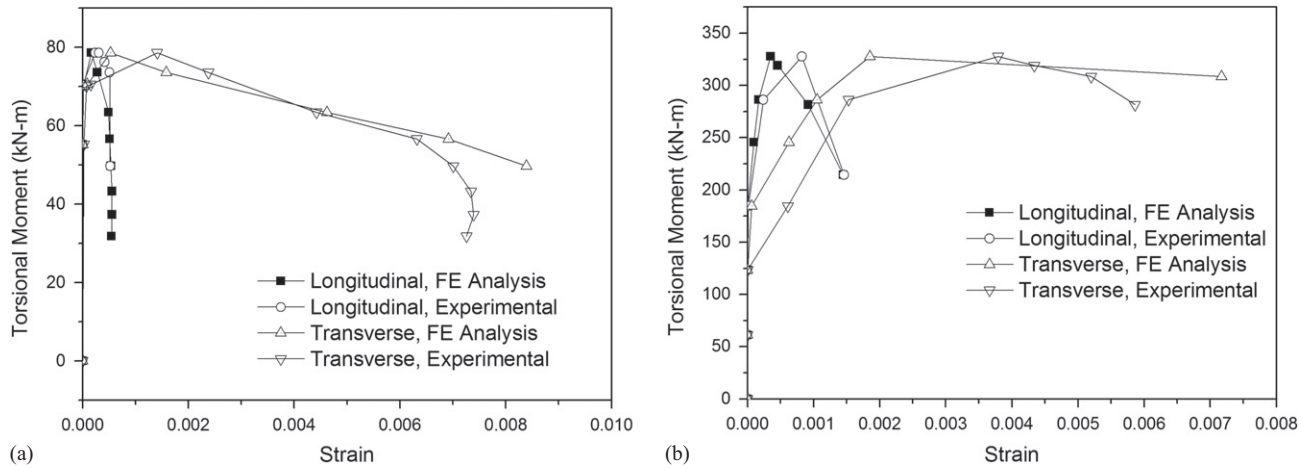

Fig. 7. Strain in the rebar: (a) TP-92; (b) H/D(3)-T/M(∞)-1.32%

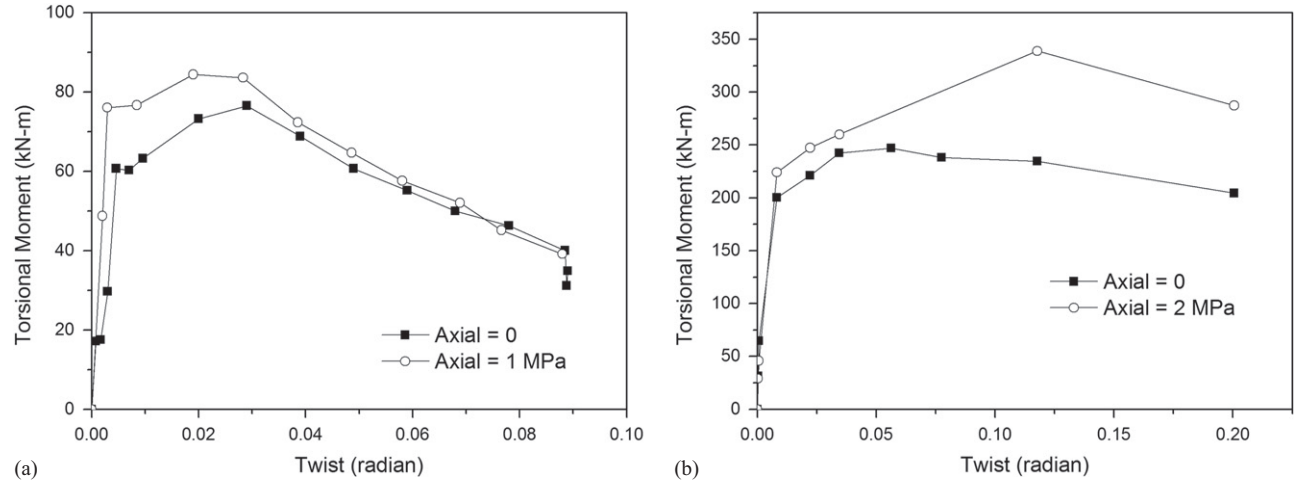

Fig. 8. Effect of axial compression: (a) square column; (b) circular column

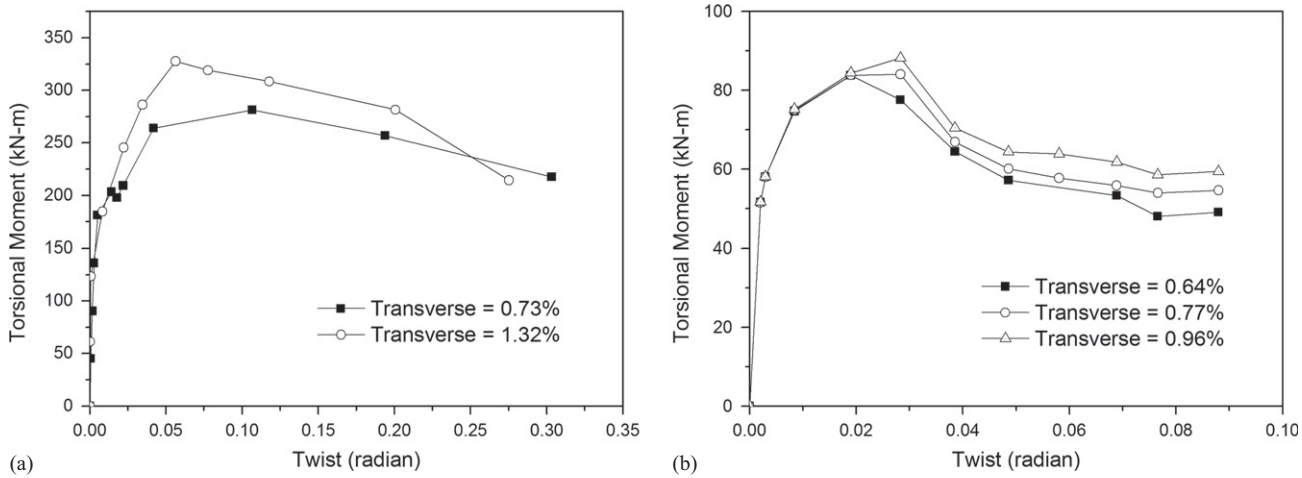

Fig. 9. Effect of transverse steel ratio on overall torque–twist behavior: (a) circular column (axial compression = 2 MPa); (b) square column (axial compressive stress = 1 MPa)

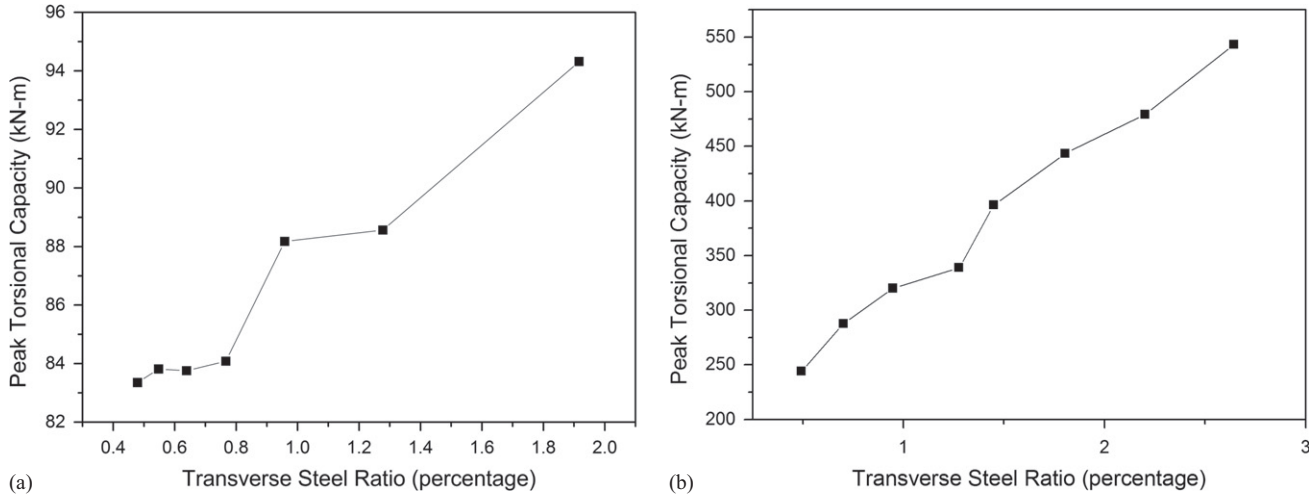

Fig. 10. Effect of transverse steel ratio on peak torsional capacity: (a) square column (axial compressive stress = 1 MPa); (b) circular column (axial compressive stress = 2 MPa)

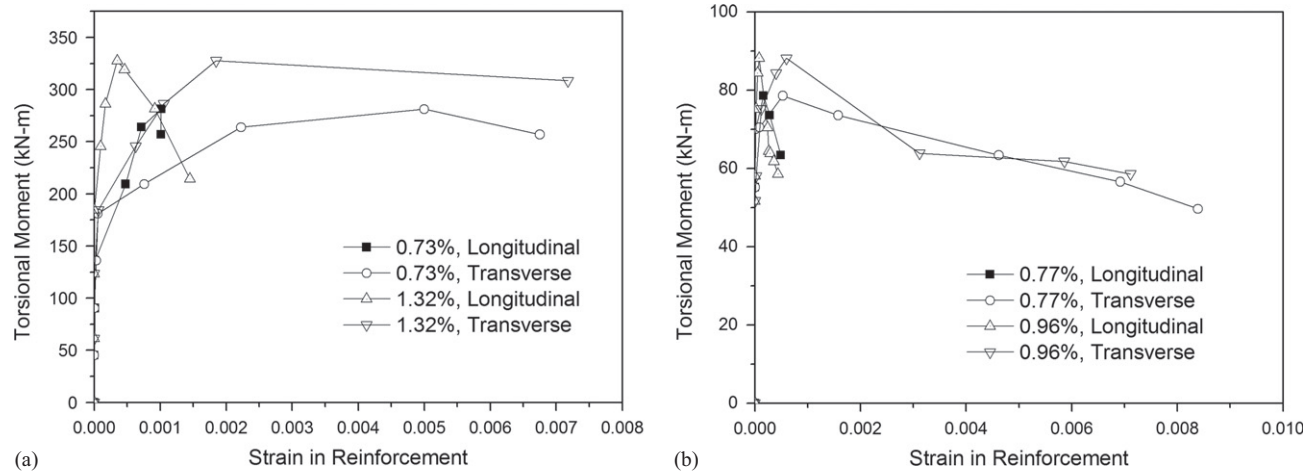

Fig. 11. Effect of transverse steel ratio on strain level in reinforcement: (a) circular column (axial compression = 2 MPa); (b) square column (axial compressive stress = 1 MPa)

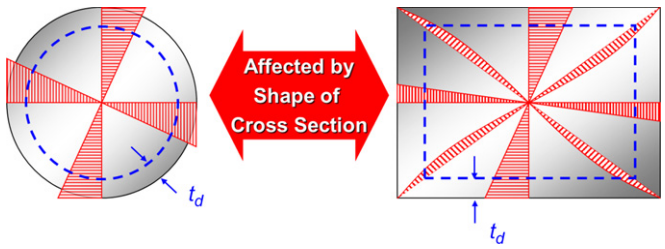

Fig. 12. Variation of shear stress for square and circular cross sections

capacity of the columns, as observed in Fig. 10. This is true because, when a RC member is cracked from applied torsion, apparent truss action is developed where the longitudinal and the transverse steel act as tensile links. Thus, the transverse reinforcements contribute to the torsional capacity of RC members. The twist at the ultimate torsional moment was increased for square columns because of increased confinement and reduced softening by transverse reinforcement. However, the value of the

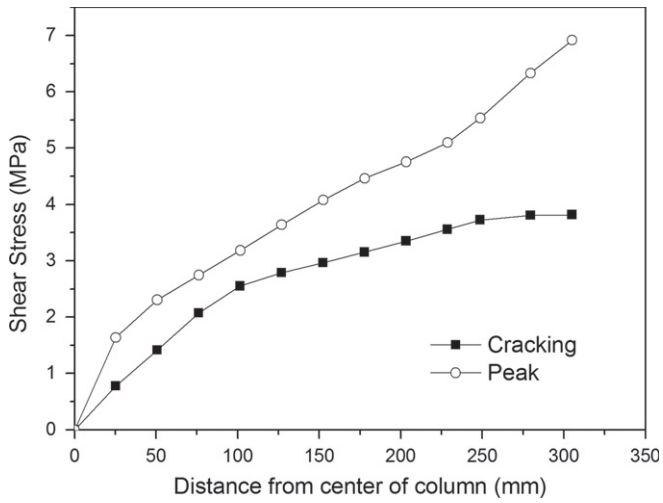

Fig. 13. Variation of shear stress due to torsion in radial direction for circular sections

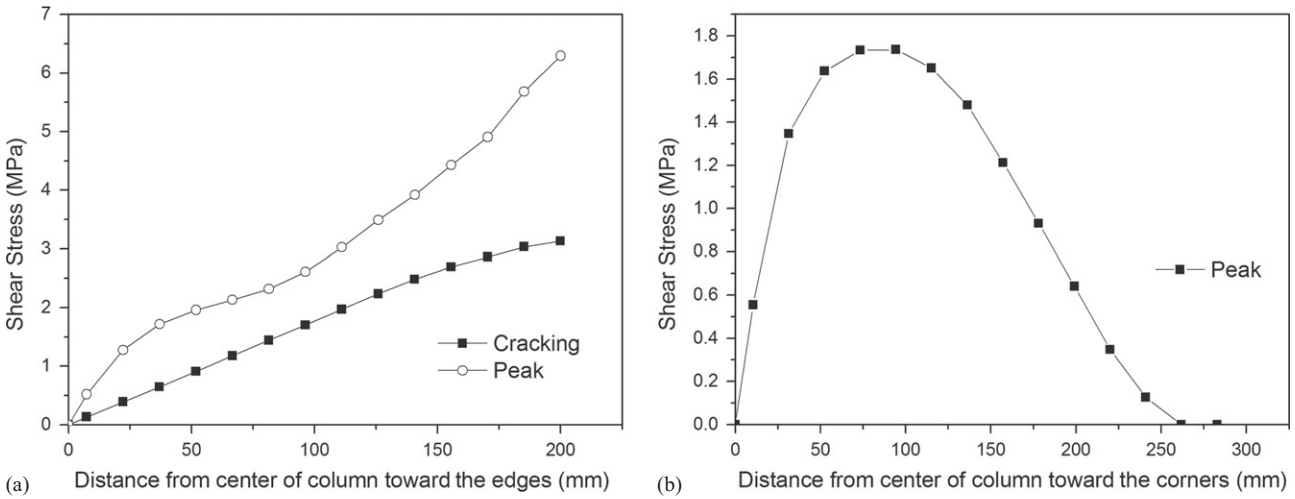

Fig. 14. Variation of shear stress due to torsion in square sections: (a) variation of shear stress toward the edges; (b) variation of shear stress in diagonal direction

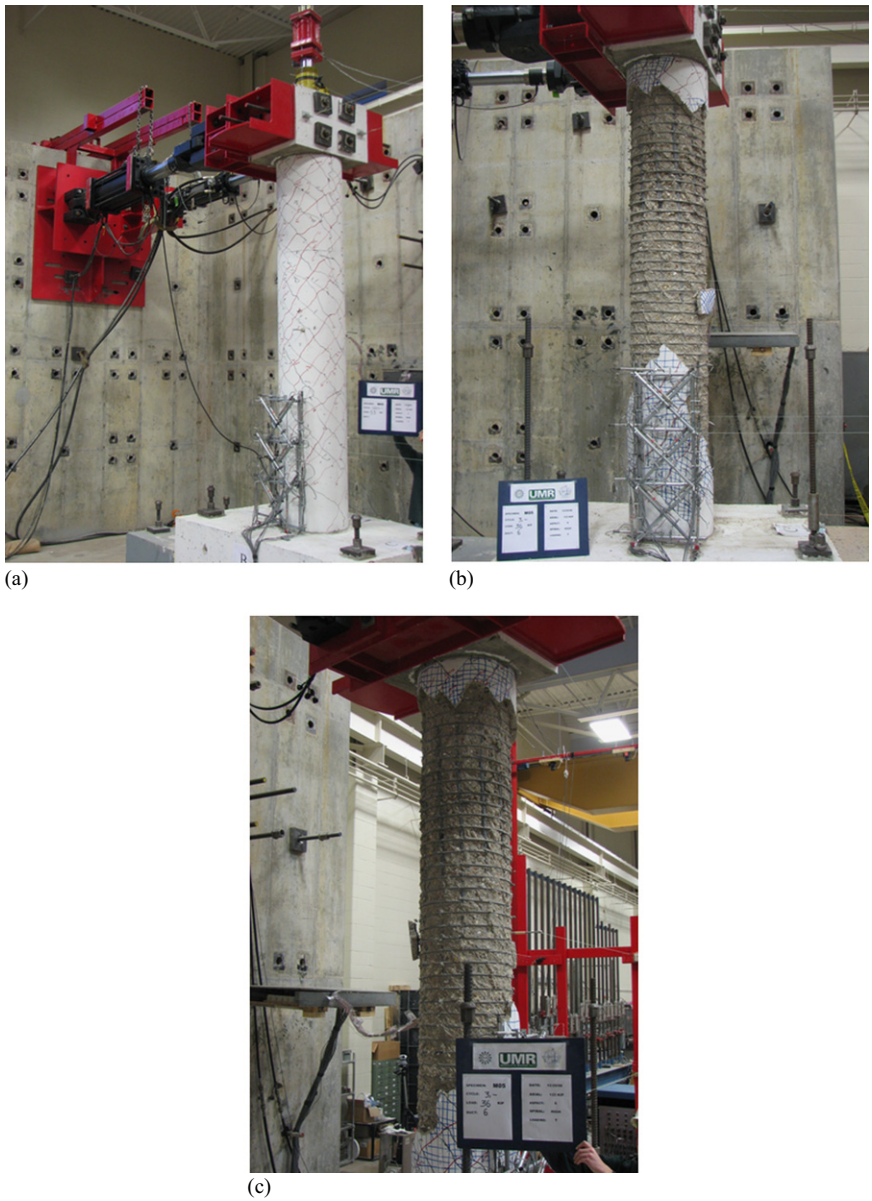

Fig. 15. Damage in circular column under pure torsion at (a) transverse bar yield; (b) peak torsional moment; (c) overall failure

same parameter was reduced for circular columns owing to the change in failure mode from ductile yield of reinforcement to brittle compressive failure of diagonal concrete strut. For square and circular columns, the variation in longitudinal and transverse strains with torsional moment for different transverse reinforcement ratio is compared in Fig. 11. It is observed that an increase in the transverse steel ratio increases the stiffness of the member, thereby limiting the strain levels in longitudinal as well as in transverse reinforcement, indicating less damage to the columns.

Thickness of Shear Flow Zone

The ultimate strength of RC members under torsion can be predicted by the truss models, the MCFT (Vecchio and Collins 1986), or the softened truss model (Hsu 1988; Pang and Hsu 1996; Hsu and Zhang 1997). These theories are based on Bredt's thin-tube theory (Bredt 1896), which assumes that the torque resisted by the section acts as shear stress flowing around the perimeter of the cross section. The concrete core of a solid member is assumed not to contribute to the torsional resistance. These theories commonly assume a RC member as assemblies of two-dimensional membrane elements, also called panels, subjected to inplane shear and normal stresses. Therefore, the behavior of a RC member under pure torsion can be predicted via the behavior of membrane elements including additional equilibrium and compatibility equations. Finite-element analysis can help to improve the predictions of these models by accurately estimating shear-flow thickness. The variation of shear stress at ultimate loads depends on the shape of the cross section. The typical distribution of shear stress for circular and rectangular cross sections is shown in Fig. 12. The predicted shear-flow distribution for circular and square columns at both the cracking and peak torsional resistance is shown in Figs. 13 and 14, respectively. The variation of shear stress was found to be highly nonlinear at peak torsional loading for both the circular and square cross sections. Higher shear stresses occured at the outer periphery of the cross section, validating Bredt's thin-tube theory. The results show that the calibrated FE models can be used for parametric studies to establish accurate estimation of shear-flow thickness for developing simple analytical models for design purpose.

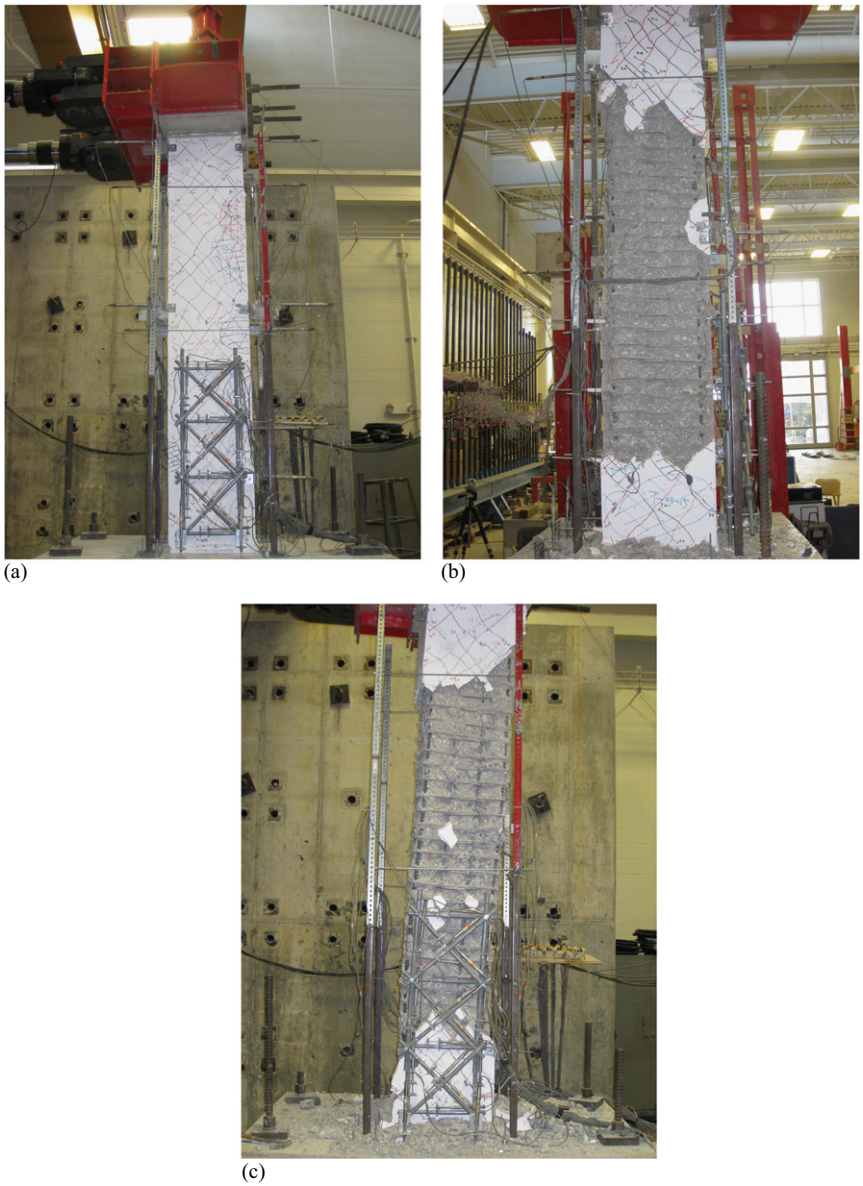

Fig. 16. Damage in square column under pure torsion at (a) transverse bar yield; (b) peak torsional moment; (c) overall failure

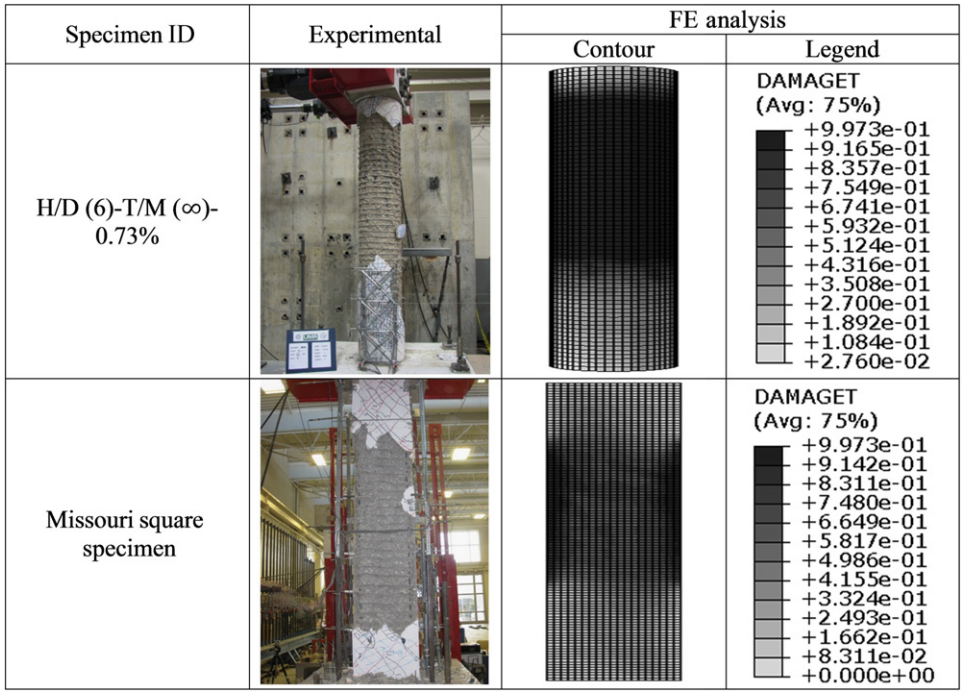

Fig. 17. Damage distribution in columns under pure torsion at final failure

Damage and Spalling of Cover

Typically, diagonal cracks start developing from near the midheight of the column under applied torsion at lower levels of loading. The cracks spread and close in the form of inclined spirals as the loading is increased. Soon after the diagonal cracking, an apparent truss action is formed where the spirals act as tensile links. After significant yielding of spirals at a high level of torsional loading, a plastic zone forms near midheight of the column. The progression of damage observed during testing is shown in Figs. 15 and 16.

The damage state observed at ultimate load showed a good correlation with the FE prediction, as shown in Fig. 17. The tensile damage variable is used in this study to quantify degradation of the material. It is a nondecreasing quantity associated with the tensile failure of the material strength. The value of this variable is zero before any degradation of the material takes place, and it reaches its maximum value of 1 at complete degradation of the material. At an intermediate level of damage, it assumes a value between 0 and 1, depending on the level of damage. In essence, this parameter represents failure of material in a structure under loading in a quantitative sense. It was further observed that the effect of cross-sectional shape played a major role in the distribution of damage in the columns. Square columns exhibited a more localized damage (Fig. 17) owing to warping deformation compared with that of circular columns, where the damage was predominantly distributed over a greater column height.

Conclusions

This paper presented the results of nonlinear FE analysis for RC columns under combined torsion and axial compression. It discussed the effects of increasing the transverse reinforcement ratio and axial compression on strength, stiffness, and damage characteristics for both square and circular columns. The effect of cross-sectional shape on the torsional behavior of RC columns was also discussed. The generated FE model exhibited excellent convergence and numerical stability characteristics, requiring little computational time for analyses under torsional loading. Within the scope of parameters considered in this study, the results lead to the following major conclusions:

- The FE model generated in this study accurately simulates the overall experimental responses of columns under combined torsion and axial compression. Strength, stiffness, ductility, damage progression, and failure modes are captured accurately. Computed parameters, such as reinforcement strains and member deformations, are also simulated well.
- At low levels of axial compression, the cracking torsional moment increases significantly, but the ultimate torsional moment increases marginally. Future studies should focus on experimentally investigating the influence of higher levels of axial compression on the torsional capacity of RC bridge columns for further validation.
- The increase in transverse reinforcement ratio increased the peak torsional strength. However, it reduced the twist component at the ultimate torsional moment. It also helps to limit the damage in columns under pure torsion.
- The effect of cross-sectional shape plays a major role in the distribution of damage in the columns. Square columns exhibited a more localized damage, whereas the same in the circular columns was distributed over a larger length.
- Finite-element analysis can help to rationally estimate the shear-flow thickness for developing simple analytical models from a design point of view. This is scope for further work.

Acknowledgments

This analytical work is carried out as part of the project funded by the Science and Engineering Research Board, the Department of Science and Technology, India. Their financial support is gratefully acknowledged. Experimental data used in this study were carried out as part of a project funded by the Network for Earthquake Engineering Simulation, the National Science Foundation, and the Network for Earthquake Engineering Simulation Research,

the National University Transportation Centre, and the Intelligent Systems Centre of the Missouri University of Science and Technology. Their financial support during the second author's Ph.D. work is also gratefully acknowledged.

References

Belarbi, A., Prakash, S., and Li, Q. (2009). "Cyclic behavior of square versus circular RC columns under combined loading including torsion." *Proc., 25th U.S.–Japan Bridge Engineering Workshop* (CD-ROM), PWRI, Tsukuba, Japan.

Bishara, A., and Peir, J. C. (1973). "Reinforced concrete rectangular columns in torsion." *J. Struct. Div.*, 94(12), 2913–2934.

Bredt, R. (1896). "Kritische bemerkungen zur Drehungselastizitat." *Z. Ver. Dtsch. Ing.*, 40(28), 785–790 (in German).

Chaudhari, S. V., and Chakrabarti, M. A. (2012). "Modeling of concrete for nonlinear analysis using finite element code ABAQUS." *Int. J. Comput. Appl.*, 44(7), 14–18.

Claeson, C., and Johansson, M. (1999). "Finite element analysis of confined concrete columns." *Proc., 5th Int. Symp. on Utilization of High-Strength/High-Performance Concrete*, I. Holand, and E. Sellevold, eds., Norwegian Concrete Association, Oslo, Sandefjord, Norway.

Delso, J. M., Stavridis, A., and Shing, B. (2011). "Modeling the bond-slip behavior of confined large diameter reinforcing bars." *III ECCOMAS Thematic Conf. on Computational Methods in Structural Dynamics and Earthquake Engineering COMPDYN*, M. Papadrakakis, M. Fragiadakis, and V. Plevris, eds., Corfu, Greece, 14.

Fink, J., Petraschek, T., and Ondris, L. (2007). "Push-out test parametric simulation study of a new sheet-type shear connector." *Projekte an den zentralen Applikationsservern, Berichte 2006*, Zentraler Informatikdienst (ZID) der Technischen Univ. Wien, Wien, Austria, 131–153.

Floros, D., and Ingason, O. A. (2013). "Modeling and simulation of reinforced concrete beams: Coupled analysis of imperfectly bonded reinforcement in fracturing concrete." Master's thesis, Dept. of Applied Mechanics, Div. of Solid Mechanics, Chalmers Univ. of Technology, Goteborg, Sweden.

Goel, R. K., and Chopra, A. K. (1994). "Seismic response of the U.S. 101/Painter Street overpassing using strong motion records." *SMIP94 Seminar on Seismological and Engineering Implications of Recent Strong-Motion Data*, M. Huang, ed., California Div. of Mines and Geology, Sacramento, CA, 75–88.

Greene, G. G. (2006). "Behavior of reinforced concrete girders under cyclic torsion and torsion combined with shear: Experimental investigation and analytical models." Ph.D. thesis, Dept. of Civil, Architectural, and Environmental Engineering, Univ. of Missouri, Rolla, MO.

Hsu, H. L., and Liang, L. L. (2003). "Performance of hollow composite members subjected to cyclic eccentric loading." *Earthquake Eng. Struct. Dyn.*, 32(3), 443–461.

Hsu, H. L., and Wang, C. L. (2000). "Flexural-torsional behavior of steel reinforced concrete members subjected to repeated loading." *Earthquake Eng. Struct. Dyn.*, 29(5), 667–682.

Hsu, T. T. C. (1968). "Torsion of structural concrete: Behavior of reinforced concrete rectangular members." *Torsion of Structural Concrete, SP-18*, American Concrete Institute, Detroit, MI, 261–306.

Hsu, T. T. C. (1988). "Softening truss model theory for shear and torsion." *ACI Struct. J.*, 85(6), 624–635.

Hsu, T. T. C., and Zhang, L. X. (1997). "Nonlinear analysis of membrane elements by fixed-angle softened-truss model." *ACI Struct. J.*, 94(5), 483–492.

Hurtado, G. (2009). "Effect of torsion on the flexural ductility of reinforced concrete bridge columns." Ph.D. thesis, Dept. of Civil and Environmental Engineering, Univ. of California, Berkeley, CA.

Isakovic, T., Fischinger, M., and Fajfar, P. (1998). "Torsional behavior of single column bent viaducts." Proc., *6th U.S. National Conf. on Earthquake Engineering (6NCEE)*, Earthquake Engineering Research Institute (EERI), Oakland, CA.

Jakobsen, B., Hjorth-Hansen, E., and Holand, I. (1984). "Cyclic torsion tests of concrete box columns." *J. Struct. Eng.*, 10.1061/(ASCE)0733-9445(1984)110:4(803), 803–822.

Jankowiak, T., and Lodygowski, T. (2005). "Identification of parameters of concrete damage plasticity constitutive model." *Found. Civ. Environ. Eng.*, (6), 53–69.

Johnson, N. S., Saiidi, M., and Sanders, D. H. (2006). "Large-scale experimental and analytical seismic studies of a two-span reinforced concrete bridge system." *CCEER Rep. No. 06-02*, Center for Civil Engineering Earthquake Research, Univ. of Nevada, Reno, NV.

Kmiecik, P., and Kamiński, M. (2011). "Modeling of reinforced concrete structures and composite structures with concrete strength degradation taken into consideration." *Arch. Civil. Mech. Eng.*, 11(3), 623–636.

McLean, D. L., and Buckingham, G. C. (1994). "Seismic performance of bridge columns with interlocking spiral reinforcement." *Rep. WA-RD 357.1*, Washington State Dept. of Transportation, Olympia, WA.

Meng, J. Y., and Lui, E. M. (2000). "Torsional effects on short-span highway bridges." *Comput. Struct.*, 75(6), 619–629.

Mitchell, D., and Collins, M. P. (1974). "Diagonal compression field theory: A rational model for structural concrete in pure torsion." *ACI J. Proc.*, 71(8), 396–408.

Mondal, T. G., and Prakash, S. S. (2015a). "Effect of tension stiffening on the behaviour of reinforced concrete circular columns under torsion." *Eng. Struct. J.*, 92, 186–195.

Mondal, T. G., and Prakash, S. S. (2015b). "Effect of tension stiffening on the behaviour of square RC columns under torsion." *Struct. Eng. Mech. J.*, 54(3), 501–520.

Mondal, T. G., and Prakash, S. S. (2015c). "Improved softened truss model for behaviour of reinforced concrete circular columns under combined torsion and axial compression." *Mag. Concr. Res.*, 67(1), 12.

Mullapudi, T. R. S., and Ayoub, A. (2009). "Non-linear finite element analysis of RC bridge columns using the softened membrane model." *Structures Congress 2009: Don't Mess with Structural Engineers: Expanding Our Role*, L. Griffis, T. Helwig, M. Waggoner, and M. Hoit, eds., ASCE, Reston, VA, 1–10.

Nagata, S., Kawashima, K., and Watanabe, G. (2004). "Seismic performance of reinforced concrete C-bent columns based on a hybrid loading test." *1st Int. Conf. on Urban Earthquake Engineering*, Tokyo, Japan, 409–416.

Nelson, R. B., Saiidi, M., and Zadeh, S. (2007). "Experimental evaluation of performance of conventional bridge systems." *CCEER Rep. No. 07-04*, Center for Civil Engineering Earthquake Research, Univ. of Nevada, Reno, NV.

Ogata, T., Suda, K., and Masukawa, J. (2000). "Transverse reinforcement and ductility of reinforced concrete high pier with hollow section." *12th World Conf. on Earthquake Engineering (12WCEE)*, Upper Hutt, New Zealand Society for Earthquake Engineering, Auckland, New Zealand.

Otsuka, H., Takeshita, E., Yabuki, W., Wang, Y., Yoshimura, T., and Tsunomoto, M. (2004). "Study on the seismic performance of reinforced concrete columns subjected to torsional moment, bending moment and axial force." *13th World Conf. on Earthquake Engineering (13WCEE)*, Vancouver, BC, Canada.

Pang, X. B., and Hsu, T. T. C. (1996). "Fixed-angle softened-truss model for reinforced concrete." *ACI Struct. J.*, 93(2), 197–207.

Prakash, S. S. (2009). "Seismic behavior of RC circular columns under combined loading including torsion." Ph.D. thesis, Dept. of Civil Engineering, Missouri Univ. of Science and Technology, Rolla, MO.

Prakash, S. S., Belarbi, A., and You, Y. M. (2010). "Seismic performance of circular RC columns subjected to axial force, bending, and torsion with low and moderate shear." *Eng. Struct. J.*, 32(1), 46–59.

Prakash, S. S., Li, Q., and Belarbi, A. (2012). "Behavior of circular and square RC bridge columns under combined loading including torsion." *ACI Struct. J.*, 109(3), 317–328.

Rabbat, B. G., and Russell, H. G. (1985). "Friction coefficient of steel on concrete or grout." *J. Struct. Eng.*, 10.1061/(ASCE)0733-9445(1985)111:3(505), 505–515.

Saadeghvaziri, M. A., and Fouch, D. A. (1990). "Behavior of RC columns under non-proportionally varying axial load." *J. Struct. Eng.*, 10.1061/(ASCE)0733-9445(1990)116:7(1835), 1835–1856.

SIMULIA (2011). *Abaqus* user's manual 6.11. Providence, RI.

Tirasit, P. (2006). "Seismic performance of reinforced concrete columns of bridges under combined flexural and torsional loading." Ph.D. thesis, Dept. of Civil and Environmental Engineering, Tokyo Institute of Technology, Tokyo.

Tirasit, P., and Kawashima, K. (2005). "Seismic torsion response of skewed bridge piers." *J. Earthquake Eng.* (CD-ROM), 116(28), 357–364.

Tirasit, P., and Kawashima, K. (2007a). "Effect of nonlinear torsion on the performance of skewed bridge piers." *J. Earthquake Eng.*, 12(3), 980–998.

Tirasit, P., and Kawashima, K. (2007b). "Seismic performance of square reinforced concrete columns under combined cyclic flexural and torsional loadings." *J. Earthquake Eng.*, 11(3), 425–452.

Vecchio, F. J., and Collins, M. P. (1986). "The modified compression-field theory for reinforced concrete elements subjected to shear." *ACI Struct. J.*, 83(2), 219–231.

Zimmermann, S. (2001). "Finite Elemente und ihre Anwendung auf physikalisch und geometrisch nichtlineare Probleme." *Rep. TUE-BCO 01.05*, Eindhoven Univ. of Technology, Eindhoven, Netherlands (in German).